PHYSICAL REVIEW B VOLUME 49, NUMBER 24 15 JUNE 1994-II

Quantum-dot quantum well CdS/HgS/CdS: Theory and experiment

D. Schooss, A. Mews, A. Eychmüller,* and H. Weller
Hahn-Meitner-Institut, Abteilung Photochemie, Glienickerstrasse 100, D-14109 Berlin, Germany

(Received 28 October 1993; revised manuscript received 23 February 1994)

An extended theoretical approach for calculating the 1*s*-1*s* electronic transition in spherically layered semiconductor quantum dots is presented. The extension over the common effective-mass approximation includes the implementation of the Coulomb interaction and finite potential wells at the particle boundaries. The calculations are carried out for the quantum-dot quantum well CdS/HgS/CdS and compared to recently available experimental results. The wave functions of electrons and holes spreading over the entire structure and the probabilities of presence in the different layers, as well as outside the structure in the surrounding dielectric water, are presented.

I. INTRODUCTION

During the past few years considerable progress has been made in the synthesis of low-dimensional semiconductor structures; that is, quantum dots of a wide variety of I-VII,[1,2] II-VI,[3-6] III-V,[7-9] and even group-IV (Refs. 10-13) semiconductors have been prepared in good quality in terms of crystallinity and size dispersivity. Some of the preparation approaches yield gram amounts of size-quantized matter.

Besides the preparation of different and improved quantum dots, other synthesis goals are the control of the particle surfaces and the buildup of more complex structures consisting of size-quantized matter. Some reports have appeared dealing with the implementation of small islands of a given semiconductor into the surface of another size-quantized particle. This work has been extended to completely coated semiconductor particles, i.e., to spherical core-shell structures.[14-23]

During the last year it has proven possible to generate three-layered quantum dots. They are composed of two semiconductor materials, of which the one with the smaller bulk band gap is embedded between a core and an outer shell of the material with the larger bulk band gap. The first examples of this family of quantum confinement exhibiting particles consist of a core of CdS (cubic, $E_{g,\mathrm{bulk}}=2.5$ eV, lattice parameter $a=5.818$ Å) spherically covered by several monolayers of β-HgS (cubic, $E_{g,\mathrm{bulk}}=0.5$ eV, $a=5.851$ Å) and several monolayers of, again, CdS acting as the outermost shell. The wet chemical synthesis, the characterization and some linear and nonlinear optical properties of these species—which, in analogy to quantum-well structures, have been named quantum-dot quantum wells (QDQW's)—have recently been reported in detail.[24-26] It has been shown that the linear absorption of the composite particles, having total diameters of between 5 and 12 nm, differs considerably from the sum of the linear absorptions of the respective subunits. Consequently, it was concluded that the composites are excited coherently, giving rise to a new band gap or 1*s*-1*s* transition. The transition energy can be tuned by the core diameter, the thickness of the well, and the thickness of the outermost shell. Theoretically the 1*s*-1*s* transition of QDQW's has been modeled in the framework of the effective-mass approximation, generally following the approaches introduced by Kortan *et al.*[19] and Haus *et al.*[27]

In this paper the model is extended in two ways: first, by the inclusion of the Coulomb interaction between the electron and the hole; and second, by the introduction of a finite potential at the edges of the particles allowing one to account for the dielectric environment. The latter extension was already discussed in Ref. 27, but the authors restricted their calculations to infinite barriers at the particle boundaries.

The outline of this paper is as follows: first, a brief overview of the general theoretical approach is given followed by the treatment of the Coulomb interaction and a description of the specific potential applied to the CdS/HgS/CdS structures in water as the dielectric environment. Section II is followed by a comparison of the experimentally and theoretically determined 1*s*-1*s* transition energies. Section IV provides some deeper insight into the shape of the wave functions, and the probability for the presence and localization of electrons and holes depending on both the well and the shell thickness.

II. THEORY

A. The general approach

The stationary Schrödinger equation for a particle under the action of a force may be expressed as

$$\left[-\frac{\hbar^2}{2}\nabla\frac{1}{m}\nabla+V(\mathbf{r})\right]\psi(\mathbf{r})=E\psi(\mathbf{r})\ , \qquad (1)$$

where $\hbar$ is Planck's constant divided by 2π, m the particle mass, ∇ the Nabla operator which is used since the mass will be treated as a radial-dependent variable, $V(\mathbf{r})$ a potential, E the energy eigenvalue, and $\Psi(\mathbf{r})$ the corresponding eigenfunction. For a spherically symmetric potential $V(\mathbf{r})=V(r)$, the separation of radial and angular coordinates leads to

$$\Psi_{nlm}(r,\theta,\phi)=R_{nl}(r)Y_{lm}(\theta,\phi)\ . \qquad (2)$$

$R_{nl}(r)$ is the radial wave function, and $Y_{lm}(\theta,\phi)$ a spherical harmonic. n is the principal quantum number, and l and m are the angular momentum quantum numbers.

For a spherical potential with the stepwise constant values V_q in N regions,

$$V(r)=\begin{cases} V_1 & \text{for } 0\le r<r_1 \\ V_2 & \text{for } r_1\le r<r_2 \\ \vdots & \\ V_N & \text{for } r_{N-1}\le r<\infty\ , \end{cases} \tag{3}$$

the radial eigenfunction $R_{nl}(r)$ consists of N parts designated $R_{nl,q}$:

$$R_{nl}(r)=\begin{cases} R_{nl,1} & \text{for } 0\le r<r_1 \\ R_{nl,2} & \text{for } r_1\le r<r_2 \\ \vdots & \\ R_{nl,N} & \text{for } r_{N-1}\le r<\infty\ . \end{cases} \tag{4}$$

Two cases need to be distinguished for the solution of $R_{nl,q}$: in regions where $E_{nl}>V_q$, the solution is a linear combination of the spherical Bessel and Neumann functions j_l and n_l:

$$R_{nl,q}(r)=A_{nl,q}j_l(k_{nl,q}r)+B_{nl,q}n_l(k_{nl,q}r)\ , \tag{5}$$

with

$$k_{nl,q}=[2m_q(E_{nl}-V_q)/\hbar^2]^{1/2} \tag{6}$$

(m_q is the effective mass of a given particle in region q).

In regions where $E_{nl}<V_q$, the solution is a linear combination of the two Hankel functions $h_l^{(+)}$ and $h_l^{(-)}$:

$$R_{nl,q}(r)=A_{nl,q}h_l^{(+)}(i\kappa_{nl,q}r)+B_{nl,q}h_l^{(-)}(i\kappa_{nl,q}r)\ , \tag{7}$$

with

$$\kappa_{nl,q}=[2m_q(V_q-E_{nl})/\hbar^2]^{1/2}\ . \tag{8}$$

The solution must satisfy the fitting conditions[28,29]

$$R_{nl,q}(r_q)=R_{nl,q+1}(r_q)\ , \tag{9}$$

$$\frac{1}{m_q}\frac{dR_{nl,q}(r)}{dr}\bigg|_{r=r_q}=\frac{1}{m_{q+1}}\frac{dR_{nl,q+1}(r)}{dr}\bigg|_{r=r_q}\ . \tag{10}$$

Together with the requirement that the solution has to be regular for $r=0$ and that it has to vanish sufficiently rapidly for $r\rightarrow\infty$, Eqs. (9) and (10) lead to a system of $2N-2$ linear equations for the $2N-2$ unknown coefficients $A_{nl,1}$, $A_{nl,2}$, and $B_{nl,2},\ldots,A_{nl,N}$. It has a nontrivial solution only if its determinant

$$D_l=D_l(E_{nl})=0\ . \tag{11}$$

Once the eigenvalue is determined as a single zero of (11), the linear equations can be solved yielding the coefficients $A_{nl,q}$ and $B_{nl,q}$ as a function of one of them. The last undetermined coefficient is fixed by the normalization condition for $R_{nl}(r)$.

We shall restrict the calculations to 1s states. Thus, for $n=1$, $l=m=0$ the spherical harmonic $Y_{0,0}(\theta,\phi)$ yields only a constant factor of $1/(4\pi)^{1/2}$.

These calculations were performed independently for electrons and holes, giving the confinement energies $E_{e,1s}$ and $E_{h,1s}$.

B. The Coulomb interaction

In a first approximation, the Coulomb interaction energy of an exciton can be treated as a heliumlike perturbation term

$$E_c=-\frac{e^2}{4\pi}\int\int d\mathbf{r}_e d\mathbf{r}_h \frac{\psi_e^*(\mathbf{r}_e)\psi_h^*(\mathbf{r}_h)\psi_e(\mathbf{r}_e)\psi_h(\mathbf{r}_h)}{|\mathbf{r}_e-\mathbf{r}_h|} \times\frac{1}{\varepsilon(r_e,r_h)}\ , \tag{12}$$

where the indices e and h refer to electrons and holes, respectively, and ε is the high-frequency dielectric constant.

For a 1s-1s exciton after expansion of $1/(|\mathbf{r}_e-\mathbf{r}_h|)$ in spherical harmonics and integration over the angular coordinates, the Coulomb energy can be written as

$$E_c=-\frac{e^2}{4\pi\varepsilon_0}\int\int dr_e dr_h r_e^2 r_h^2 \frac{|R_e(r_e)|^2|R_h(r_h)|^2}{\max(r_e,r_h)} \times\frac{1}{\bar{\varepsilon}_r(r_e,r_h)}\ , \tag{13}$$

where $\bar{\varepsilon}_r(r_e,r_h)$ is the mean relative dielectric constant of the material between the electron and the hole.[30]

The sum of the confinement energies, the Coulomb energy and the bulk band-gap energy of the material with the larger band gap gives the new band gap of the composite material:

$$E_{\text{gap}}=E_{e,1s}+E_{h,1s}+E_c+E_{\text{gap,macro}}\ . \tag{14}$$

This bulk band gap must be added, since the confinement energies of the electrons and holes are calculated relative to the valence- and conduction-band positions of the semiconductor material with the larger bulk band gap.

C. The potential

In Fig. 1 the appropriate potential for describing the prepared QDQW's is depicted. From left to right one sees the CdS core for $0\le r<r_1$, the HgS well for $r_1\le r<r_2$, the outer CdS shell for $r_2\le r<r_3$ and the dielectric water for $r\ge r_3$. (We chose $r=3r_3$, i.e., three times the total particle radius as the cutoff for the Coulomb calculations). The absolute band positions of water were taken from Watanabe and Gerischer,[31] and the conduction-band potential for CdS from Ref. 32. The band offset, i.e., the difference between the conduction-band positions of CdS and HgS, were calculated according to Nethercot[33] with the use of electronegativity data. The physical parameters are $E_{g,\text{CdS}}=2.5$ eV and $E_{g,\text{HgS}}=0.5$ eV, the effective masses $m_{e,\text{H}_2\text{O}}=m_{h,\text{H}_2\text{O}}=1$, $m_{e,\text{CdS}}=0.2$, $m_{h,\text{CdS}}=0.7$, $m_{e,\text{HgS}}=0.036$, and $m_{h,\text{HgS}}=0.044$, and the high-frequency dielectric constants

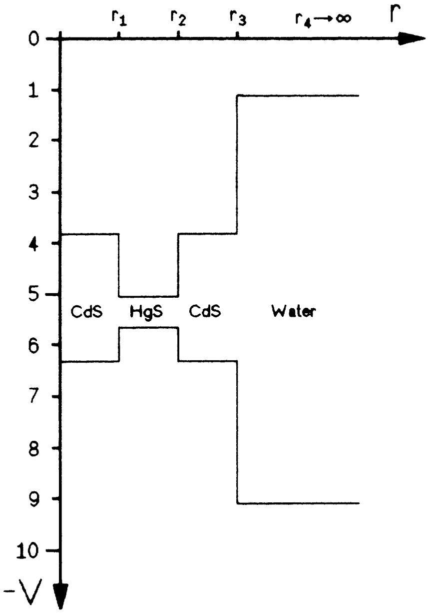

FIG. 1. Potential for the description of CdS/HgS/CdS QDQW's in water.

$\varepsilon_{H_2O}=1.78$, $\varepsilon_{CdS}=5.5$, and $\varepsilon_{HgS}=11.36$.[34,35] The iterative calculations were terminated when the variation of the energies remained within 10^{-5} eV.

III. COMPARISON EXPERIMENT—THEORY

Before presenting the results of the calculations, a brief comment about the course of the preparation of the QDQW's should be made. The starting CdS colloidal particles have an average diameter of 5.3 nm. By the addition of Hg^{2+} ions to this solution, a substitution reaction takes place: the surface Cd^{2+} ions are replaced by Hg^{2+} ions yielding particles with a 4.7-nm CdS core and a 0.3-nm surface layer of HgS. A QDQW consisting of a 4.7-nm CdS core, one layer of HgS, and (almost) one layer of CdS as the outermost shell is prepared by precipitating by H_2S the Cd^{2+} ions present in solution after the preceding substitution reaction. The HgS well thickness is increased by repetition of the substitution and precipitation steps. The outermost CdS shell thickness may be increased by the addition of Cd^{2+} ions and H_2S to a given solution of CdS/HgS/CdS particles. This course of preparation was followed by electron microscopy, polarography, and mass spectrometry as outlined in detail in Ref. 26.

An overview of the QDQW's prepared so far is given in Table I. The absorption spectra of the samples labeled *a*–*g* are shown in Fig. 2. Spectrum *a* is that of pure CdS particles of 5.3-nm diameter; spectrum *b* of particles with a 4.7-nm CdS core and a 0.3-nm surface layer of HgS; and spectrum *c* of the first QDQW consisting of the 4.7-nm CdS core, a 0.3-nm, HgS well, and an outermost shell of 0.3 nm of CdS. Spectrum *d* shows the absorption of particles with a 4.7-nm CdS core covered by 0.6 nm of HgS, and spectrum *e* evolves by capping these particles with 0.3 nm of CdS. The particles giving spectrum *f* have a 4.7-nm CdS core and three layers of HgS, i.e., 0.9 nm. Finally, these particles are covered by a monolayer of CdS giving spectrum *g*.

Together with the absorption spectra we depicted some results of the calculations according to Eq. (14), for the 1*s*-1*s* transition energy of QDQW's. It can be seen that the bars indicating the results of the calculations match the experimentally obtained ones quite well. (The points of maximum curvature in the absorption spectra are a good measure for the 1*s*-1*s* transition energies.[36]) Thus the agreement between experiment and theory is good enough to allow the conclusion that the model describes QDQW's in a reasonable manner. This although satisfying, is somewhat surprising, keeping in mind the simplicity of the model and the expected breakdown of the effective-mass approximation for structures as small as

TABLE I. Summary of the compositional data of the prepared particles together with the energy of the 1*s*-1*s* electronic transition ("band gap") as determined experimentally and theoretically with infinite barriers and finite barriers at the particle boundaries. Column 8 gives the Coulomb interaction energy. "Band-gap theoret." was calculated according to Eq. (14).

Sample	CdS core diameter [nm]	HgS layer thickness [nm]	CdS layer thickness [nm]	Total particle diameter [nm]	Band-gap inf. Pot. [eV]	Band-gap fin. Pot. [eV]	Coulomb interact. [meV]	Band-gap theoretical [eV]	Band-gap measured [eV]
a	5.3	0	0	5.3	2.84	2.74	−154	2.59	2.62
b	4.7	0.3	0	5.3	2.92	2.53	−121	2.41	2.56
c	4.7	0.3	0.3	5.9	2.71	2.35	−84	2.27	2.10
	4.7	0.3	1.0	7.3	2.30	2.25	−76	2.16	1.96
	4.7	0.3	1.5	8.3	2.25	2.23	−75	2.15	1.94
d	4.7	0.6	0	5.9	2.91	2.10	−69	2.03	1.91
e	4.7	0.6	0.3	6.5	2.32	1.88	−58	1.83	1.76
f	4.7	0.9	0	6.5	2.89	1.72	−50	1.67	1.70
g	4.7	0.9	0.3	7.1	1.93	1.57	−48	1.53	1.60
	4.7	0.9	1.5	8.0	1.55	1.55	−48	1.50	1.55
	4.7	0.9	2.2	8.7	1.55	1.55	−48	1.50	1.54

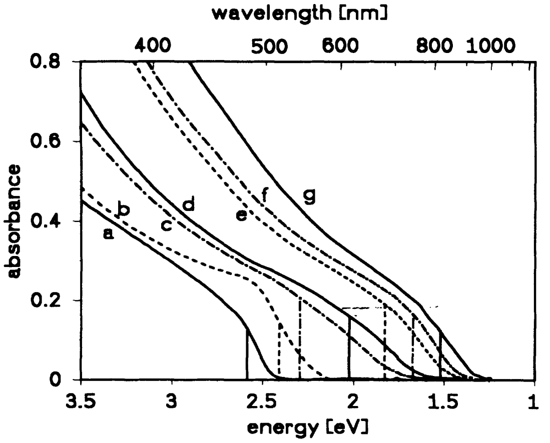

FIG. 2. Absorption spectra of CdS/HgS/CdS QDQW's of various compositions compared to theoretical results; cf. text.

one monolayer, as well as the uncertainties in experimentally characterizing the prepared particles. However, similarly good results were obtained with the effective-mass approximation applied to quantum wells in which the wells were also as thin as one monolayer.[37] We are thus convinced that the model presented above gives at least a very good first impression of the 1s-1s transition energy of QDQW's. The inclusion of the Coulomb interaction and the introduction of a finite potential at the edges of the particles successfully removes the discrepancy of about 200 meV observed between experimentally and theoretically determined 1s-1s transition energies without these refinements.[26]

In Fig. 3 we plotted the whole set of results of the calculations according to Eq. (14). We depicted the 1s-1s transition energies for particles with 4.7-nm CdS cores surrounded by up to three monolayers of HgS (0.9 nm) and up to three monolayers (0.9 nm) of CdS. The particles which have been synthesized are also indicated. The labeling (a–g) is as above, and the dashed lines follow the preparative course of increasing the outer CdS layer thickness at given HgS layer thicknesses. The starting point of the preparation is a pure CdS colloid of 5.3-nm diameter (a). The surface substitution reaction yields particles having a 4.7-nm CdS core capped by a 0.3-nm HgS layer (b). Steps $b \rightarrow c$, $d \rightarrow e$, and $f \rightarrow g$ represent the coverage of given CdS/HgS particles by an outer shell of CdS, and steps $c \rightarrow d$ and $e \rightarrow f$ the increase in HgS layer thickness by one monolayer each. From Fig. 3 it can be seen that the gap energy decreases rapidly with increasing HgS layer thickness compared to an increase in CdS layer thickness. The following result is probably the most remarkable: tracing a graph of constant HgS layer thickness and increasing CdS shell thickness (e.g., from d via e along the dashed line) one notices that the gap energy decreases. In other words, by capping a given CdS/HgS composite by the large band-gap material CdS ($E_{\mathrm{gap,bulk}}=2.5$ eV) the new 1s-1s transition energy in the QDQW drops below even the 1s-1s transition energy of the CdS/HgS composite. This effect is observable only in quantum-confined material, and can be understood by a more detailed analysis of the results presented in Sec. IV.

Before that, a brief inspection is made of how the inclusion of finite barriers and the Coulomb interaction into the theoretical treatment influences the results of the calculations. For this, in Fig. 4 the results of the calculations are plotted as a function of the HgS and CdS layer thicknesses (A) with infinite barriers and without Coulomb interaction, (B) with finite barriers at the particle boundaries, still without Coulomb interaction; and (C) including both extensions of the theoretical approach (as in Fig. 3). The results for the particles actually prepared are given in Table I, columns 6–9. Keeping in mind that plane (C) fits the experimental data reasonably well, it can be clearly seen from Fig. 4 that the introduction of finite potential wells at the particle boundaries is essential for a good theoretical approximation of the 1s-1s transition energies in QDQW's. This is seen most

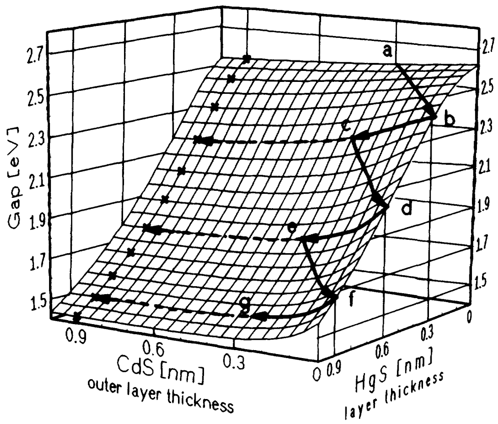

FIG. 3. Calculated 1s-1s transition energies of QDQW's with 4.7-nm CdS cores as a function of HgS and CdS shell thicknesses. The labeling a–g is as in Fig. 2; the crosses correspond to particles whose charge-carrier wave functions are shown in Fig. 5.

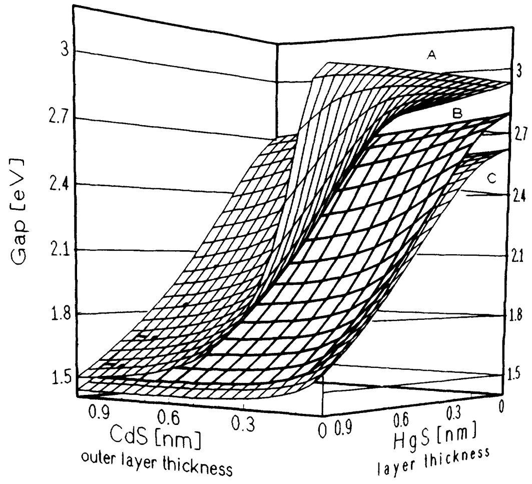

FIG. 4. Calculated 1s-1s transition energies for QDQW's with 4.7-nm CdS cores as a function of HgS and CdS shell thicknesses. (A) with infinite barriers, neglecting the Coulomb interaction; (B) with finite barriers, neglecting the Coulomb interaction; and (C) same as Fig. 3, including Coulomb interaction and finite barriers at the particle boundaries.

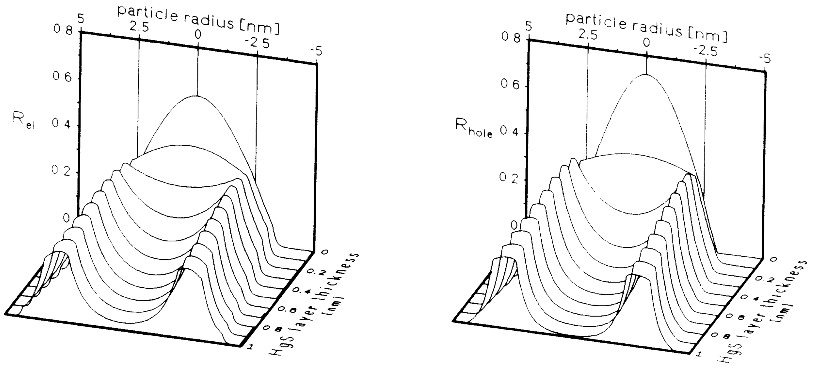

FIG. 5. Radial wave functions of the electrons (a) and holes (b) in QDQW's with a 4.7-nm CdS core, 0.9-nm outer CdS shell, and variable HgS well thickness (corresponding to the crosses in Fig. 3).

dramatically for particles without CdS as the outermost shell: whereas the actual 1*s*-1*s* transition energies for particles with a CdS core capped by one, two, and three monolayers of HgS (samples *b*, *d*, and *f*) drop by about 740 meV with increasing number of layers the theoretically derived energies with infinite barriers remain constant at about 2.9 eV. Obviously, the infinite barrier prevents the charge carriers from relaxing into the HgS wells.

The influence of the Coulomb interaction is less drastic. The inclusion of this force in the theoretical treatment yields a decrease of the 1*s*-1*s* transition energy of 154 meV for pure CdS particles with a diameter of 5.3 nm. For the largest particles under consideration this decrease amounts to 48 meV, which at the present state of the preparative techniques is more or less insignificant. This situation may change provided that the preparation and characterization of QDQW's will be refined in the future. In this case, polarization effects also should be included in a theoretical treatment. These effects are expected to be on the order of one-third of the Coulomb interaction,[38,39] but with a positive sign.

IV. WAVE FUNCTIONS AND PROBABILITY OF PRESENCE

In this concluding section three specific features are inspected in somewhat more detail, namely the wave functions, the probability of presence in the different compartments of particles, and the probability of presence of electrons and holes outside the particles in the surrounding medium. In Fig. 5 the radial wave functions (without the perturbation introduced by the Coulomb interaction) for the electron (left) and hole (right) are plotted for particles having 4.7-nm CdS cores, variable HgS layer thickness, and a coverage of three layers of CdS as the outer shell. For pure CdS the *s*-like Gaussian-shaped wave functions for both electrons and holes are recognizable. Both maxima are found at the center of the particles at $r=0$. Due to the larger effective mass compared to that of the electron, the amplitude of the hole wave function is somewhat larger at $r=0$. For both charge carriers the amplitude in the middle of the particles decreases rapidly with increasing HgS layer thickness. Already at a coverage of as little as 0.2 nm the amplitude of the wave function of the hole is larger in the HgS moiety than the CdS core. This effect is less dramatic for the electron. Even at well thicknesses of about 1 nm the wave function of the electron is spread wider over the whole particle including a certain amplitude even in the outer CdS shell [cf. Fig. 5(a)]. These pictures vary to a certain extent with the core diameter and the CdS shell thickness, but the general features do not change significantly. In all combinations of radii (except for one; see below) studied so far, the hole wave function was found to have higher amplitudes in the well region than the electron wave function. Furthermore, a set of radii can be determined exhibiting a pronounced charge-carrier separation.

In order to obtain an even better impression of where the charge carriers are to be found in the particles, the radial probability of presence $\int R^2 r^2 dr$ must be calculated. This has been done for electrons and holes, and the results are plotted in Fig. 6 as a function of both HgS and the outer CdS layer thickness. Again, the CdS core was taken to be 4.7 nm.

From Figs. 6(a) and 6(b) it can be seen that for pure

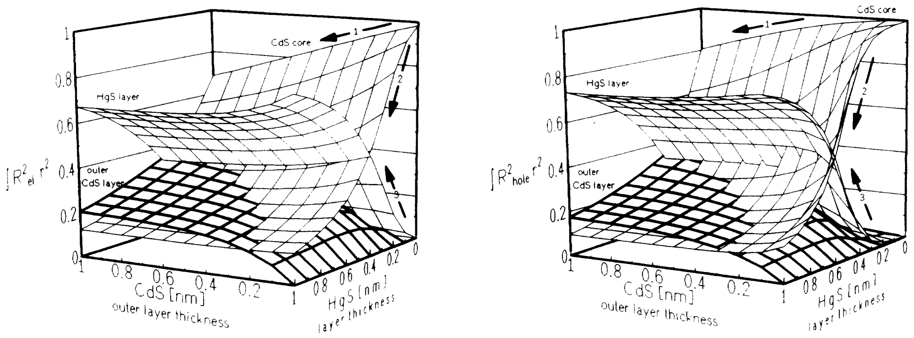

FIG. 6. The probability of presence of electrons (a) and holes (b) in QDQW's with a 4.7-nm CdS core as a function of HgS and CdS shell thicknesses. For the arrows, cf. text.

CdS (back, top) an increase in diameter leads to a decrease in the probability of presence in the core (arrow 1), i.e., the *s*-like wave functions spread more widely over the entire particles. Trivially, this is accompanied by an increase in finding the charge carriers further apart from the center of the particles. The loss of probability of presence in the core is drastically enhanced by covering the core by HgS instead of CdS, as seen by tracing the CdS core graphs from the right back top along the HgS axis to the front (arrow 2). Even at very small coverages, the charge carriers are localized at the surface of the particles in the HgS moiety (arrow 3). An interesting feature is that for these CdS/HgS composites (without an outer CdS shell) the electrons are already localized at smaller coverages in the HgS than the holes. This is reversed for all other compositions, as mentioned above. Another not easily predictable observation is seen by tracing the topmost graph for the HgS well of 1-nm thickness in Fig. 6(a): at low CdS coverages the probability of presence in the HgS well is high, and decreases with increasing CdS capping (i.e., the electrons "leak out" into the CdS shell). To a smaller extent this is also seen for the holes in Fig. 6(b). Together, these results show that if one is to design QDQW structures with desired properties such as strong localization for one or both charge carriers, or as the most pronounced charge carrier separation, an analysis of this kind may be useful before attempting a synthesis of the particles.

The last topic to be discussed is how the probability of finding electrons and/or holes outside the particles depends on the particle composition. In order to answer this question we plotted $\int_{r_3}^{\infty} R^2 r^2 dr$ as a function of both HgS and CdS layer thicknesses in Fig. 7. As expected from the above considerations, it was found that thick CdS outer layers prevent the charge carriers from escaping from the particles, since they are "pushed" into the well by the shell material with the larger band gap. In cases without surrounding CdS, the probability of finding electrons and holes outside the particles is higher the higher the charge-carrier density (i.e., the probability of presence divided by the volume) in the HgS moiety. This is most pronounced for the electrons at 0.4-nm HgS, and for the holes at 0.6-nm coverage. In this context it is worth mentioning that the QDQW's fluoresce stronger the thicker the outer CdS shell is at a given HgS well thickness. This has been understood in terms of the closing of channels of radiationless transitions at the HgS surfaces by capping with CdS. With the results of the calculations concerning the probability of presence of the charge carriers outside the particles, this charge transfer to the surrounding dielectric might very well be assigned to one of the radiationless processes deactivating the particles and preventing them from fluorescing.

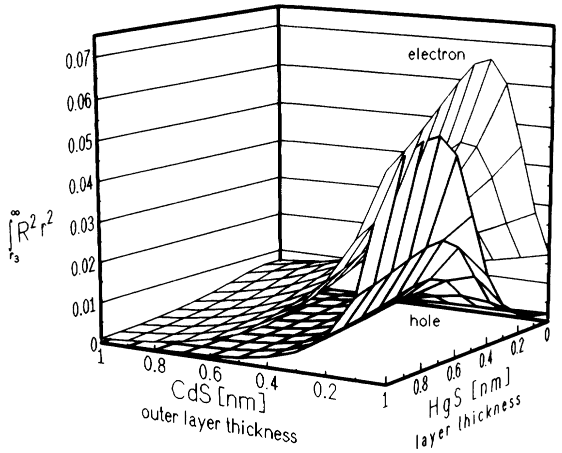

FIG. 7. The probability of the presence of electrons and holes outside the particles as a function of the composition (CdS core diameter: 4.7 nm).

Further work on QDQW's will focus on the dynamics and energetics of the charge carriers as a function of temperature, where fluorescence will be used as the probe. The synthesis goals of the near future are the preparation of multiply layered structures hopefully giving multiple-quantum-dot quantum wells, and the use of other materials than CdS and HgS. In finding good combinations of materials theoretical considerations such as the one presented here will probably be of great help.

ACKNOWLEDGMENTS

Thanks are due to Dr. Ivanka Popovic for carefully reading the manuscript and to G. Priebe for helpful discussions.

---

[*] Author to whom correspondence should be addressed.

[1] A. Nakamura, H. Yamada, and T. Tokizaki, Phys. Rev. B **40**, 8585 (1989).

[2] A. Nakamura, T. Tokizaki, H. Akiyama, and T. Kataoka, J. Lumin. **53**, 105 (1992).

[3] For reviews, see A. Henglein, Pure Appl. Chem. **56**, 1215 (1984); L. E. Brus, IEEE J. Quantum Electron. **22**, 1909 (1986); J. Phys. Chem. **86**, 2555 (1986); A. Henglein, Top. Curr. Chem. **143**, 115 (1988); Chem. Rev. **89**, 1861 (1989); Y. Wang and N. Herron, J. Phys. Chem. **95**, 525 (1991); H. Weller, Angew. Chem. **105**, 43 (1993); Int. Ed. **32**, 41 (1933); Adv. Mater. **5**, 88 (1993); H. Weller, A. Eychmüller, R. Vogel, L. Katsikas, A. Hässelbarth, and M. Giersig, Isr. J. Chem. **33**, 107 (1993).

[4] N. Herron, J. C. Calabrese, W. E. Farneth, and Y. Wang, Science **259**, 1426 (1993).

[5] A. Chemseddine and H. Weller, Ber. Bunsenges. Phys. Chem. **97**, 636 (1993).

[6] C. B. Murray, D. J. Norris, and M. G. Bawendi, J. Am. Chem. Soc. **115**, 8706 (1993).

[7] M. A. Olshavsky, A. N. Goldstein, and A. P. Alivisatos, J. Am. Chem. Soc. **112**, 9438 (1990).

[8] H. Ushida, C. J. Curtis, and A. J. Nozik, J. Phys. Chem. **95**, 5382 (1991).

[9] H. Uchida, C. J. Curtis, P. V. Kamat, K. M. Jones, and A. J. Nozik, J. Phys. Chem. **96**, 1156 (1992).

[10] Y. Maeda, N. Tsukamoto, Y. Yazawa, Y. Kanemitsu, and Y. Masumoto, Appl. Phys. Lett. **59**, 3168 (1991).

[11] J. R. Heath, Science **258**, 1131 (1992).

[12] K. A. Littau, P. J. Szajowski, A. J. Muller, A. R. Kortan, and L. E. Brus, J. Phys. Chem. **97**, 1224 (1993).

[13] A. Kornowski, M. Giersig, R. Vogel, A. Chemseddine, and H. Weller, Adv. Mater. **5**, 634 (1993).

[14] H. Weller, U. Koch, M. Gutiérrez, and A. Henglein, Ber. Bunsenges. Phys. Chem. **88**, 649 (1984).

[15] L. Spanhel, H. Weller, A. Fojtik, and A. Henglein, Ber. Bunsenges. Phys. Chem. **91**, 88 (1987).

[16] L. Spanhel, M. Haase, H. Weller, and A. Henglein, J. Am. Chem. Soc. **109**, 5649 (1987).

[17] H. C. Youn, S. Baral, and J. H. Fendler, J. Phys. Chem. **92**, 6320 (1988).

[18] A. Henglein, M. Gutiérrez, H. Weller, A. Fojtik, and J. Jirkovsky, Ber. Bunsenges. Phys. Chem. **93**, 593 (1989).

[19] A. R. Kortan, R. Hull, R. L. Opila, M. G. Bawendi, M. L. Steigerwald, P. J. Carroll, and L. E. Brus, J. Am. Chem. Soc. **112**, 1327 (1990).

[20] C. F. Hoener, K. A. Allan, A. J. Bard, A. Campion, M. A. Fox, T. E. Mallouk, S. E. Webber, and J. M. White, J. Phys. Chem. **96**, 3812 (1992).

[21] A. Eychmüller, A. Hässelbarth, and H. Weller, J. Lumin. **53**, 113 (1992).

[22] H. S. Zhou, I. Honma, H. Komiyama, and J. W. Haus, J. Phys. Chem. **97**, 895 (1993).

[23] A. Hässelbarth, A. Eychmüller, R. Eichberger, M. Giersig, A. Mews, and H. Weller, J. Phys. Chem. **97**, 5333 (1993).

[24] A. Eychmüller, A. Mews, and H. Weller, Chem. Phys. Lett. **208**, 59 (1993).

[25] A. Eychmüller, T. Vossmeyer, A. Mews, and H. Weller, J. Lumin. **58**, 223 (1994).

[26] A. Mews, A. Eychmüller, M. Giersig, D. Schooss, and H. Weller, J. Phys. Chem. **98**, 934 (1994).

[27] J. W. Haus, H. S. Zhou, I. Honma, and H. Komiyama, Phys. Rev. B **47**, 1359 (1993).

[28] D. J. Ben Daniel and C. B. Duke, Phys. Rev. **152**, 683 (1968).

[29] L. E. Brus, J. Chem. Phys. **79**, 5566 (1983).

[30] For the calculation of the "mean dielectric constant" the fraction of material i located between the electron and hole was determined, weighted with the corresponding dielectric constant ε_i, and finally summed over all i. In principle, the dielectric constants in each part of the composites could be used explicitly (as a referee suggested). This would increase the numerical expense enormously since a sum of up to 16 double integrals instead of one would have to be calculated and, additionally, the numerical accuracy would have to be enhanced.

[31] T. Watanabe and H. Gerischer, J. Electroanal. Chem. **122**, 73 (1981).

[32] A. Hässeelbarth, A. Eychmüller, and H. Weller, Chem. Phys. Lett. **203**, 271 (1993).

[33] A. H. Nethercot, Phys. Rev. Lett. **33**, 1088 (1974).

[34] I. Broser, R. Broser, M. Rosenzweig, and G. Nimtz, in *Zahlenwerte und Funktionen aus Naturwissenschaften und Technik,* edited by O. Madelung, M. Schulz, and H. Weiss, Landolt-Börnstein, New Series, Group III, Vol. 17, Pt. b (Springer-Verlag, Berlin, 1982), Secs. 3.10.1 and 3.14.B.1.

[35] B. F. Bilen'kii, R. V. Gerasimchuk, M. V. Kurik, and M. V. Pashkovskii, Izv. Vyssh. Ucheb. Zaved. Fiz. **12**, 157 (1969) [Sov. Phys. J. **12**, 973 (1969)].

[36] L. Katsikas, A. Eychmüller, M. Giersig, and H. Weller, Chem. Phys. Lett. **172**, 201 (1990).

[37] H. Zajicek, P. Juza, E. Abramof, O. Pankratov, H. Sitter, M. Helm, G. Brunthaler, W. Faschinger, and K. Lischka, Appl. Phys. Lett. **62**, 717 (1993).

[38] L. E. Brus, J. Chem. Phys. **80**, 4403 (1984).

[39] Y. Nosaka, J. Phys. Chem. **95**, 5054 (1991).